JOURNAL OF SPACECRAFT AND ROCKETS
Vol. 43, No. 3, May–June 2006

Transverse Vibration Analysis for Partly Wrinkled Membranes

N. M. A. Hossain* and C. H. Jenkins†
South Dakota School of Mines and Technology, Rapid City, South Dakota 57701
K. Woo‡
Chungbuk National University, Chungbuk 361-763, Republic of Korea
and
H. Igawa§
Japan Aerospace Exploration Agency, Tokyo 181-0015, Japan

The development is reported of a membrane-based wrinkle algorithm to analyze the transverse vibration behavior of partly wrinkled, annular, and three-sided membranes. This membrane-based wrinkle algorithm was implemented in the nonlinear finite element code ABAQUS, providing implementation of a true membrane constitutive model. First, the models were validated either with analytical solutions or experimental results. Then, the transverse vibration behavior of unwrinkled membrane models was studied. Finally, the presented constitutive model was incorporated in ABAQUS to inspect how wrinkling affects the vibration behavior of membranes. The frequency and mode shapes were investigated between the unwrinkled and wrinkled membranes. It was observed that even small amounts of wrinkling can significantly affect the modal frequencies of membranes. We offer physical explanation for these results.

Nomenclature

A = area
a = hub radius
b = wrinkle radius
$[C]$ = compliance matrix
$[D]$ = damping matrix
d = cable diameter
E = Young's modulus
f = frequency
h = thickness
$[K]$ = stiffness matrix
M = twisting moment
$[M]$ = mass matrix
m = $\cos(\theta_w)$
n = $\sin(\theta_w)$
R = membrane radius
S = tension per unit length
$[T]$ = transformation matrix
α = thermal expansion coefficient
γ = shear strain
ε = normal strain
$\varepsilon_{\max}$ = maximum principal strain
θ = deviation angle from unwrinkled configuration to wrinkled configuration
θ_w = angle between material and wrinkle coordinates
λ = nondimensional frequency parameter
μ = eigenvalue
ν = Poisson's ratio
ρ = density
σ = normal stress
$\sigma_{\min}$ = minimum principal stress
σ_0 = uniform radial stress
$\{\phi\}$ = eigenvector
ω = circular frequency

Subscripts and Superscripts

A = area
E = elastic
G = geometric
i = integers
j = integers
m = membrane
ov = overlaid material

Introduction

MEMBRANE structures represent thin three-dimensional surfaces that provide significant load resistance only in the direction tangential to their surface. Idealized or true membrane structures are two-dimensional surfaces having zero bending stiffness because of their negligible thickness. Wrinkling is an elastic displacement response to compressive loading of the membrane. Wrinkling is the membrane form of plate or shell buckling, an instability caused by insufficient bending stiffness.[1] Wrinkles manifest themselves as nominally sinusoidal waves in elastic sheets, which are membranes with small but nonnegligible bending stiffness.[2]

Wagner is credited as the first to analyze wrinkling.[3] He introduced a suitable solid mechanics model known as tension-field theory for analyzing membrane structures under the wrinkling condition. The tension-field theory is based on the assumption that wrinkles are oriented in the direction of the local major principal stress, and the minor principal stress in the wrinkling region, which is perpendicular to the load path, is zero. Reissner modified Wagner's theory by suggesting separate elastic moduli associated with each principal direction.[4] Steigmann and Pipkin[5] showed that true membranes are continuously wrinkled, that is, the wrinkle wavelength is zero.

Different techniques have been introduced for wrinkling analysis of membrane, which can be categorized into two major groups: deformation tensor modification and stiffness/compliance modification. The deformation tensor modification method was used by Roddeman et al.,[6,7] Kang and Im,[8] Lu et al.,[9] Nakashino and Natori.[10] The stiffness/compliance modification method was first

Received 4 June 2004; revision received 26 May 2005; accepted for publication 6 June 2005.

*Research Assistant, Mechanical Engineering Department, 501 East Saint Joseph Street. Student Member AIAA.
†Professor, Mechanical Engineering Department; currently Professor and Head, Mechanical and Industrial Engineering Department, 220 Roberts Hall, Montana State University, Bozeman, MT 59717. Associate Fellow AIAA.
‡Associate Professor, Department of Structural Systems and CAE. Member AIAA.
§Researcher, Institute of Space Technology and Aeronautics, 6-13-1 Osawa, Mitaka-City.

used by Miller et al.[11] They devised a stiffness modification method based on a variable Poisson's ratio and used this to study partly wrinkled flat membranes. (Reference 11 contains several typographical errors, which do not support the comparison of their results with modern numerical solutions. Stein and Hedgepeth did detailed analysis of partly wrinkled rectangular membranes,[12] and Mikulas extended this work, providing experimental details for a stretched annular membrane wrinkled by rotation of an attached hub.[13] Both are helpful in using the results presented in Ref. 11.) Liu et al. introduced a penalty parameter based stiffness/compliance modification method to study membrane wrinkling.[14] Jenkins and coworkers were the first to measure,[2] then verifiably predict,[15] the finite wrinkle parameters of elastic sheets, namely, the number, wavelength, and height of the wrinkles.

Adler et al. used cable-network models to analyze membrane wrinkling.[16] The cable-network modeling method is an approximate approach based upon the observation that wrinkles in flat membranes tend to run in straight lines. The basic idea was to use rod elements to create a net-like structure that approximates the mass distribution and load paths caused by wrinkling. Tessler et al. carried out the wrinkling analysis of membranes using non-linear shell modeling.[17] Wrinkling formation in membranes was studied for in-plane shear loading and symmetric corner tensile loading. Wong et al. performed the prediction of wrinkle amplitudes in square solar sails.[18] Kukathasan and Pellegrino investigated the vibration behavior of plane rectangular membrane structures subjected to different corner tensile loading.[19] Geometrically nonlinear postbuckling shell analyses were performed in Refs. 17–19, where highly meshed shell elements were used with random geometrical imperfection to instigate out-of-plane wrinkling deformation.

Future spacecraft, such as solar sails, will require ultra-low-mass structures with an extensive use of membranes.[20] Therefore, the understanding of dynamic behavior of membrane structures becomes vital for their attitude control and intended performance. Wrinkling in those structures can impact mission success in a number of important ways, ranging from degradation in performance to catastrophic structural collapse. To date, several static analyses of membrane wrinkling have been performed, but dynamic analysis of wrinkled membranes is little reported. Although Refs. 17 and 19 report on the dynamic analysis of wrinkled membranes, the membrane was modeled either using cable-network approach or standard thin shell elements available in ABAQUS. Because of the bending rigidity of shell elements, shell elements are unable to represent true membrane characteristics when the thickness is extremely low and loadings are complex. Furthermore, shell element analysis is computationally more expensive than membrane analysis.

This paper presents the dynamic analysis of partly wrinkled membranes, where the membrane surface was defined by using triangular and quadrilateral membrane elements having zero bending rigidity. A penalty-parameter-modified-material (PPMM) model, introduced earlier by Liu et al.,[14,15] was incorporated in ABAQUS for correct analysis of wrinkling. The PPMM model is a robust and accurate representation of membrane wrinkling at minimal computational cost.

The layout of this paper is as follows. First, a brief review of membrane wrinkling analysis and the current wrinkled algorithm is outlined. Second, a linear eigenvalue analysis is carried out to obtain the vibration frequencies and mode shapes of unwrinkled annular and three-sided membrane models. Geometrically nonlinear static analysis is included before eigenvalue extraction when the membrane is prestressed. Numerical solutions are compared with known closed-form or experimental values to represent the reliability of ABAQUS dynamic analysis. Finally, the PPMM model is used in ABAQUS to investigate how wrinkling effects the transverse vibration behavior. The results are then compared for similar modes of vibration between the unwrinkled and wrinkled membranes. A discussion of the results concludes the paper wherein we offer a physical explanation for the observed results.

Analysis

A membrane could be in one or more of taut, slack, or wrinkled (tension field) states based on its stress and strain state. The mixed-mode criteria (based on both principal stresses and strains) are the correct criteria for judging the membrane state.[14,21] The mixed-mode wrinkling criteria indicate the following for a membrane element:

$$\begin{aligned} &\text{If} \quad \sigma_{\min} > 0, \quad \text{the membrance is in a taut state} \\ &\text{If} \quad \varepsilon_{\max} \le 0, \quad \text{the membrance is in a slack state} \\ &\text{If} \quad \sigma_{\min} \le 0 \quad \text{and } \varepsilon_{\max} > 0, \text{ the membrance is in a wrinkled state} \end{aligned} \tag{1}$$

A robust tension field model was developed and incorporated within the nonlinear finite element code ABAQUS as a subroutine UMAT (user material). A penalty parameter was used to assign a near-zero stiffness ("penalize" the stiffness) in the direction of minimum in-plane principal stress. A small nonzero stiffness normal to the wrinkled direction was maintained to avoid the singularity problem in the stiffness matrix, which offered a converged solution of the membrane model when wrinkles exist. The PPMM approach is instigated by the physics of membrane wrinkling and is therefore a high-fidelity model. In the wrinkled state, the algorithm determines the principal directions first to develop the transformation matrices. To enforce the wrinkling criteria, the stiffness matrix is modified by a penalty parameter. The penalized stiffness matrix is then transformed back to material coordinates for calculation of elemental stresses. A flowchart is provided in Fig. 1 for a clear understanding of the wrinkle algorithm.

The PPMM model was validated by comparing the numerical solutions for stress distribution and the extent of the wrinkle region to two closed-form results involving partly wrinkled flat membranes.[12,13] This verification was presented in detail in Ref. 22, where high agreement was found between numerical and analytical results. Only a brief summary of validation against the Stein and Hedgepeth closed-form solution is included here for completeness. Numerical results are compared with the analytical solutions involving a partly wrinkled rectangular membrane model (50×25 mm), as shown in Fig. 2. A linear finite element (FE) analysis was performed because the closed-form solutions are themselves linear.

The surface of this membrane model was simulated by eight nodes parabolic membrane elements (M3D8) with the following material properties: membrane modulus $E_m = 2.8$ GPa, Poisson's ratio $\nu = 0.3$, uniform biaxial stress $\sigma_0 = 1$ MPa, and membrane thickness $h = 25\ \mu$.

The membrane is uniformly pretension with normal stress σ_0 in the y direction and with axial force $P = \sigma_0 Bh$ in the x direction. After stretching the membrane in the x and y directions, an in-plane bending moment M is applied. Increasing the moment results in a band of wrinkles of width b formed in the lower edge of the membrane.

The comparison of axial stress σ_x between the numerical and analytical solution is shown in Fig. 3 for three different loading cases. The comparison of wrinkle band b between the numerical and analytical solution is shown in Fig. 4.

These comparisons demonstrate the validation of PPMM model for wrinkling analysis of membrane structures, where high accuracy is observed.

Offering an extensive collection of solid mechanics models in their finite element libraries, no commercial finite element code includes the correct or robust tension field model for membrane wrinkling analysis. Wrinkling in membranes results from the absence of material/structural stiffness perpendicular to the wrinkle direction, with an attendant redistribution of stress in the load-carrying direction. Correct tension field models will minimize the minimum in-plane principal stress when wrinkles occur. A material option called "no compression" (NC), available in ABAQUS and other codes, generally modifies the linear elasticity so that compressive stress cannot be generated. Usually, it offers convergence difficulties unless each element that uses the NC option is overlaid with another element that uses a small value of Young's modulus E_{ov} (Ref. 23). Although this option could diminish the negative stresses from global x and y directions, it cannot correctly implement the mixed-mode criteria nor correctly predict the redistributed stress field when wrinkles exist.

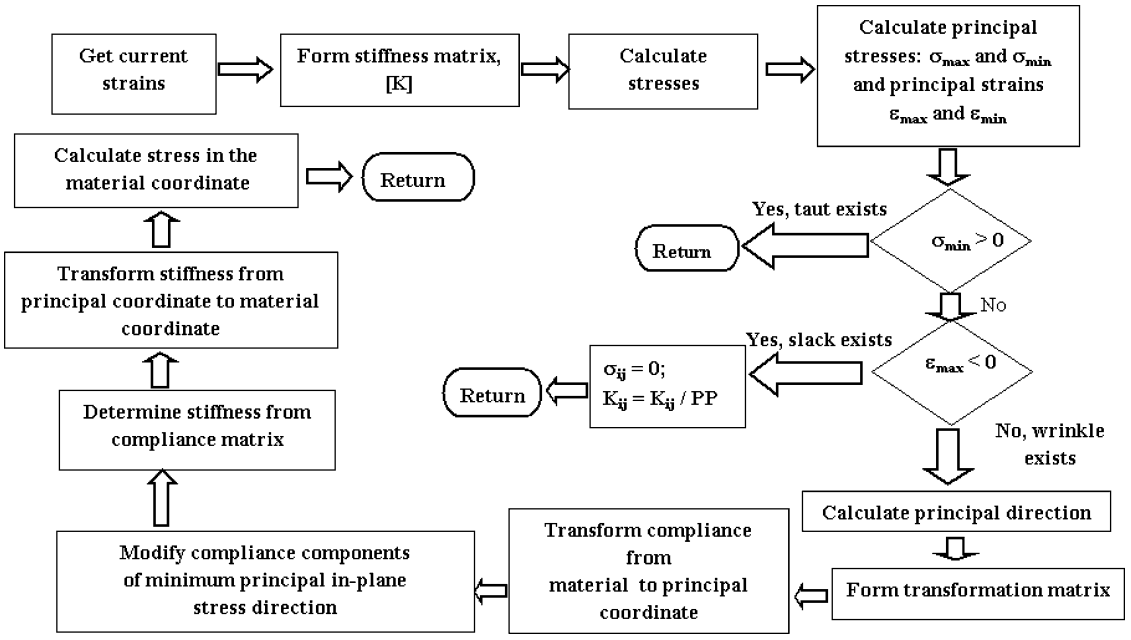

Fig. 1 Flowchart of wrinkle algorithm in ABAQUS, using UMAT subroutine.

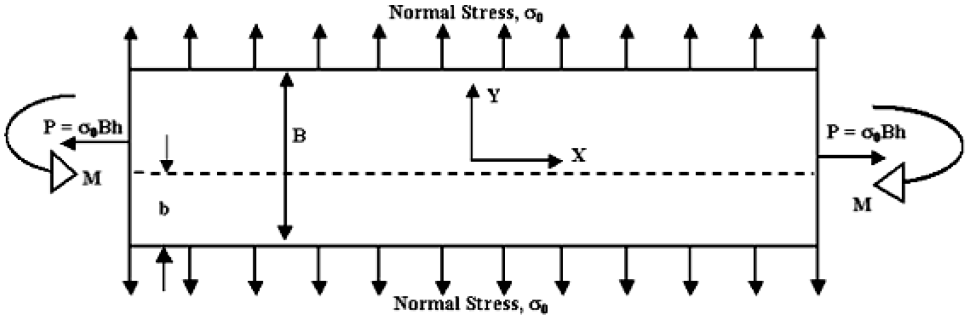

Fig. 2 Partly wrinkled rectangular membrane model under pure bending.

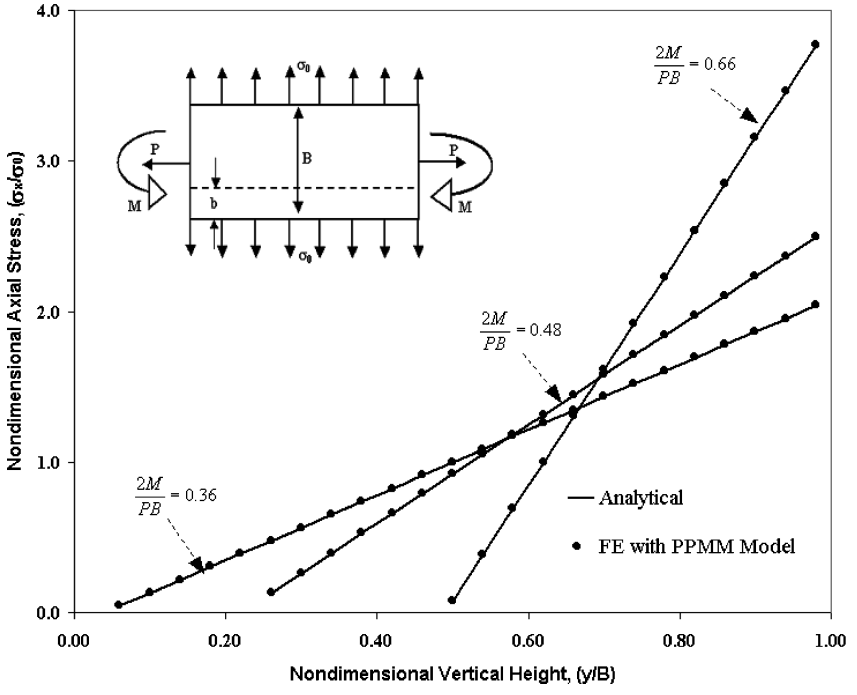

Fig. 3 Comparison of axial stress of partly wrinkled rectangular membrane under pure bending.

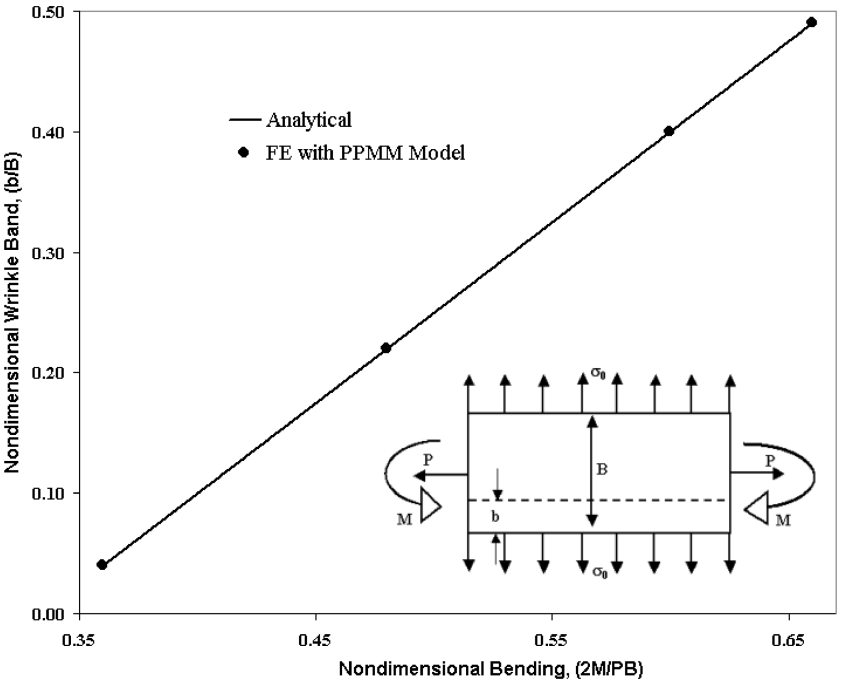

Fig. 4 Comparison of wrinkle band for party wrinkled rectangular membrane under pure bending.

In addition, the tension field cannot be correctly implemented in finite element codes by using fully implemented shell elements. Any loading or boundary conditions that evoke even the slightest moment response will allow the shell solution to deviate from the membrane solution; a polymer film of a few micron thickness is much closer to a true membrane than a shell. A postbuckling shell analysis is bending stiffness driven and, although useful for qualitative estimates of wrinkle details, is not a reliable predictor for the membrane tension field.

For many structural analyses, it is essential to extract the eigenvalues of the system, in order to ascertain vibration behavior (natural frequencies, mode shapes, damping, etc.) or investigate the possible bifurcations that might be associated with kinematic instabilities.[24] Much work has been devoted for providing the eigenvalue extraction methods. The eigenvalue problems arising out of finite element models are a particular case: they involve large but usually narrowbanded symmetric matrices, and only small number of eigenpairs is usually required. The eigenvalue problem for natural modes of small vibration of a finite element model is shown in Eq. (2) in classical matrix form:

$$(\mu^2[M] + \mu[D] + [K])\{\phi\} = 0 \tag{2}$$

where $[M]$ is symmetric and positive definite in the problems of interest. The stiffness matrix can include "stress-stiffening" initial stress terms (in the case of large displacements), and therefore $[K]$ might not be always positive definite or symmetric. In general, the stiffness matrix can be written as follows:

$$[K] = [K_E] + [K_G] \tag{3}$$

where $[K_E]$ and $[K_G]$ indicate the elastic and geometric stiffness, respectively. The elastic stiffness is independent of the initial stress state or loading, and it has a strong effect on the in-plane vibration modes. On the other hand, the geometric stiffness varies with the initial stress state or loading, and it has significance for the transverse vibration modes. (The effect of elastic stiffness $[K_E]$ on the transverse vibration is minimal but not negligible.) A finite element structure model with geometric stiffness capability usually results in a higher or lower frequency when it is subject to tensile or compressive loading, respectively, than without that effect included.

A wrinkled membrane, analyzed by the PPMM model, will exhibit the following two characteristics during dynamic analysis.

1) The PPMM model will diminish the elastic stiffness K_E of the wrinkled region and consequently reduce the total stiffness and frequency of the structure. These expected results were found for the in-plane vibration analysis of wrinkled membranes.

2) Geometric stiffness of the structure will vary with changes of the load. Because of this geometric stiffness, the taut region of the wrinkled membrane will tend to offer higher frequency if the tension in that region has increased. Because the compressive stresses of the wrinkled region will be reduced by the wrinkle algorithm, the geometric stiffness will again raise the frequency of the structure.

The eigensystem [Eq. (2)] in general has complex eigenvalues and eigenvectors. This system can be symmetrized by assuming that $[K]$ is symmetric and by neglecting $[D]$ during eigenvalue extraction. Problems examined in the following sections of this paper were carried out without considering damping. The symmetrized system then produces real squared eigenvalues μ^2 and real eigenvectors only. In this case μ becomes an imaginary eigenvalue, $\mu = i\omega$, and the eigenvalue problem can be written as

$$(-\omega^2[M] + [K])\{\phi\} = \{0\} \tag{4}$$

Results and Discussion

Transverse Vibrations of a Partly Wrinkled Annular Membrane

Consider a rigid circular hub of radius a, which is attached to a flat stretched circular membrane of radius R and thickness h comprised of 400 quadrilateral membrane elements (M3D4), as shown in Fig. 5. Uniform radial stress σ_0 is then applied to tension the annular membrane before applying pure twisting moment M at the center of the rigid hub. Membrane properties are given in Table 1. For sufficient large twisting moment M, the stress state of the annular membrane will offer an exterior taut region and an interior wrinkled region of radius b. The transverse vibration behavior of this annular membrane model has been examined for different wrinkle regions and compared with the unwrinkled membrane.

The static wrinkle analysis of this problem was performed in ABAQUS using the PPMM model and full details are provided in Ref. 22. The FE results were compared to the analytical solution in Ref. 13, and a sample of the validation results is given in Table 2.

The unwrinkled vibration problem with zero twisting moment was first considered. The analytical relation for extracting natural

frequencies is given in Ref. 25. Natural frequencies are calculated by using Eq. (5):

$$\lambda_{ij} = \frac{1}{\pi^{0.5}}\left[4j^2\left(\frac{R-a}{R+a}\right) + i^2\pi^2\left(\frac{R+a}{R-a}\right)\right]^{0.5}$$

$$f_{ij} = \frac{\lambda_{ij}}{2}\left(\frac{S}{\rho_A A}\right)^{0.5} \tag{5}$$

where ρ_A is the area density, $i = 1, 2, 3 \ldots$ and $j = 0, 1, 2 \ldots$ correspond to the different modes of vibrations, λ_{ij} is the nondimensional frequency parameter, and f_{ij} represents the frequency in hertz. The mode shapes of the annular membranes are described by two integers i and j, which represent the number of nodal (zero displacement) circles and diameters, respectively; examples are shown in Fig. 6.

For further clarification, Fig. 7 shows the first symmetric mode of annular membrane model ($i = 1$, $j = 0$). The first few transverse vibration modes of unwrinkled membrane were observed and are shown in Fig. 8.

The comparison between the numerical and analytical solution is presented in Table 3. High agreement is found between the numerical and analytical solutions with average difference of less than 3%, which is acceptable in engineering analysis.

Although the numerical accuracy could be improved by h or p refinement at increased computational cost, we take as an acceptable baseline a numerical accuracy of three parts in 100.

The dynamic analyses of the partly wrinkled annular membrane model were performed with various twisting moments that resulted in a wrinkled area characterized by $b/R = 20$ to 50%. Table 4 shows the frequencies for $b/R = 20\%$, analyzed with and without the wrinkle algorithm. Here, mode numbers indicate the modes of the unwrinkled membrane as shown in Table 3. Similar modes of vibration between the unwrinkled and wrinkled model were identified by visual observation of nodal lines (indicated by integer i and j) and by calculating the modal-assurance-criteria (MAC) number between the two cases.[26] To ensure similar modes of vibration for the two different models, MAC numbers close to 1 are desired.

The wrinkled membrane was found to offer reduced frequencies compared to the unwrinkled membrane model when the PPMM wrinkle algorithm was not used in the analysis (see Tables 3 and 4). This is expected as the hub moment creates compressive stress in the membrane. The PPMM wrinkle algorithm diminishes the elastic stiffness normal to the wrinkle direction, therefore reducing the compressive stress in the wrinkled region. As a result, frequencies of the similar modes of vibration of the partly wrinkled annular membrane model were found to increase when the wrinkle algorithm was used during its analysis (see Table 4). The stress distribution

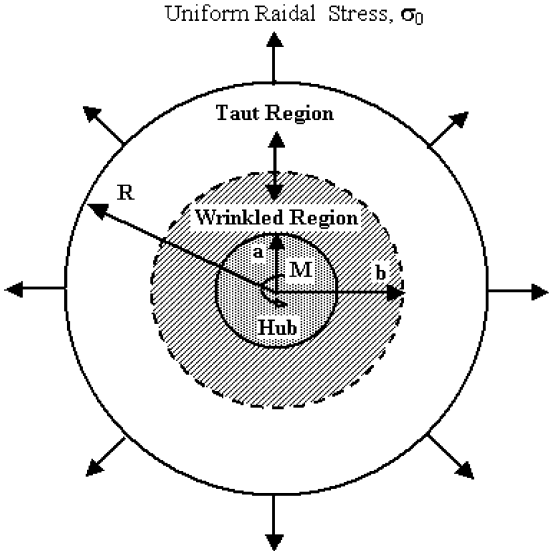

Fig. 5 Wrinkling of a flat stretched annular membrane.

Table 1 Model parameters for extracting natural frequency of the annular membrane model shown in Fig. 5

Model parameters/properties	Dimension/values
Hub radius a	0.05 m
Outer radius R	0.5 m
Membrane thickness h	25 μm
Membrane modulus E	2.72 GPa
Membrane density ρ	1440 kg/m^3
Uniform initial tension σ_0	7.78 MPa

Table 3 Frequency comparison between analytical and numerical solution for annular membrane model

Mode (i, j)	Analytical, Hz	Numerical, Hz	% Difference[a]
1 (1, 0)	2.607	2.471	5.03
2 (1, 1)	2.940	2.936	0.13
3 (1, 2)	3.766	3.831	−1.72
4 (1, 3)	4.838	4.753	1.75
5 (2, 0)	5.215	5.109	1.97
6 (2, 1)	5.389	5.461	−1.33
7 (1, 4)	6.026	5.660	6.07
8 (2, 2)	5.881	6.301	−7.14
9 (2, 3)	6.619	6.934	−4.98
10 (3, 0)	7.823	7.735	1.23
11 (3, 1)	7.941	8.011	−0.88
12 (3, 2)	8.265	8.317	−0.62
13 (3, 3)	8.803	8.723	0.91

[a]Average difference = 2.59.

Table 4 Frequency comparison of wrinkled membrane model for $b/R = 20\%$, analyzed with and without the wrinkle algorithm[a]

	Analyzed without wrinkle algorithm		Analyzed with wrinkle algorithm	
Mode (i, j)	Frequency	MAC	Frequency	MAC
1 (1, 0)	2.468	0.994	2.755	0.994
2 (1, 1)	1.646	0.944	2.775	0.943
3 (1, 2)	3.716	0.967	3.805	0.967
4 (1, 3)	4.605	0.974	4.656	0.974
5 (2, 0)	5.043	0.983	5.576	0.960
6 (2, 1)	4.008	0.903	5.210	0.983
7 (1, 4)	5.436	0.961	5.491	0.904
8 (2, 2)	5.942	0.944	6.262	0.944

[a]Mode number conforms to Fig. 8, and MAC comparison is to the $b/R = 0$ case.

Table 2 Sample of validation for partly wrinkled annular membrane model[a]

Moment $\bar{M}$	Analytical wrinkle width, b/a	FE wrinkle width, b/a	% Error	Analytical minor principal stress, $\sigma_{\min}/\sigma_0$	FE minor principal stress, $\sigma_{\min}/\sigma_0$	% Error
2	1.471	1.437	2.31	0.983	0.976	0.71
6	2.983	2.885	3.28	0.998	0.992	0.61
9	3.789	3.699	2.37	1.021	1.014	0.68
12	4.363	4.242	2.77	1.047	1.041	0.57

[a]Quantities are the nondimensional values. Stress values are reported at nondimensional radius (r/a) of 0.75.

Table 5 Change in frequencies between the unwrinkled and wrinkled membrane model[a]

	Wrinkled membrane analyzed with PPMM algorithm			
	$(b/R = 20\%)$		$(b/R = 50\%)$	
Mode (i, j)	Frequency, Hz	% Difference	Frequency, Hz	% Difference
1 (1, 0)	2.755	11.490	4.407	78.372
2 (1, 1)	2.775	2.289	3.663	28.970
3 (1, 2)	3.805	0.619	4.779	26.374
4 (1, 3)	4.656	0.140	5.152	10.796
5 (2, 0)	5.576	10.46	8.914	76.586
6 (2, 1)	5.210	1.02	7.922	53.593
7 (1, 4)	5.491	0.49	5.601	2.498
8 (2, 2)	6.262	2.192	9.163	49.527

[a]Mode number conforms to Fig. 8.

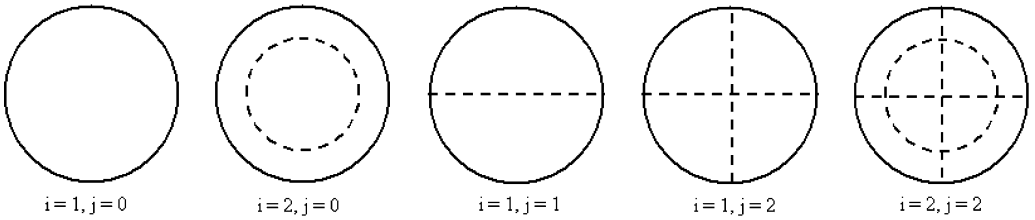

Fig. 6 Example mode shapes of an annular membrane.

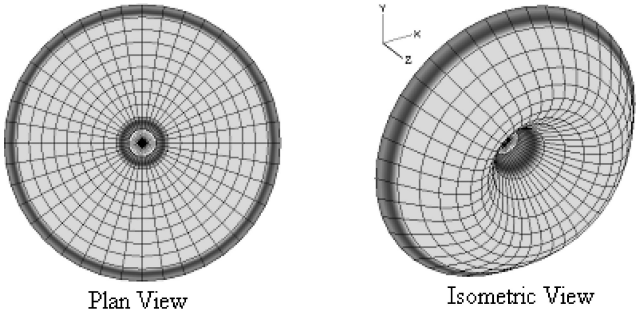

Fig. 7 First symmetric mode of vibration of annular membrane model.

of a membrane model will be altered by the extent and orientation of wrinkles. Consequently, the MAC number for the corresponding modes of vibrations between the unwrinkled and wrinkled model reasonably deviate from one.

Table 5 shows the change in frequency for the vibration modes, between the unwrinkled and wrinkled membranes for wrinkle radius of 20 and 50%. Symmetric modes of vibration, modes 1 and 5 as shown in Fig. 8, were found to change significantly. The change in frequencies for the antisymmetric modes of vibrations, modes with $(j \neq 0)$ as shown in Fig. 8, was found to be much smaller. Similar trends were observed between the unwrinkled and wrinkled membranes at any wrinkle radius. In the wrinkled model with $b/R = 50\%$, the change in frequency for the antisymmetric modes was found to be decreasing with increasing nodal diameters. The modal participation along the vibration plane was found higher for the symmetric modes of vibration compared to the antisymmetric modes. Therefore, the symmetric modes of vibration offered a more significant change in frequencies between the unwrinkled and wrinkled configurations. Although at $b/R = 20\%$, the percentage difference is often within the "noise" of the baseline numerical accuracy, by $b/R = 50\%$, the results are an order of magnitude or more greater than the baseline. Thus we consider the results numerically significant.

A twisting moment M was applied at the hub center to initiate wrinkles. Increasing the wrinkle radius by applying a higher twisting moment intensifies the radial tension of the taut region. At the same time, the wrinkle algorithm also reduces the elastic stiffness and compressive stresses of the wrinkled section. Therefore, frequencies for the similar vibration modes (having MAC number higher than 0.90 with each other) were found to increase with increasing wrinkle radius, which is shown in Figs. 9 and 10. Some complex behavior was observed for the higher-order antisymmetric mode $(i = 1, j = 4)$ when their frequency was changing with increasing wrinkled radius. Frequency was found to decrease at a wrinkle radius of 40% before it finally increased. It seems that at $b/R = 40\%$, the reduction of elastic stiffness was dominant rather than the increase in geometric stiffness in these modes.

Transverse Vibrations of Three-Sided Membrane

An experimental and analytical study to determine the basic vibration behaviors of a an equilateral three-sided membrane model, shown in Fig. 11 with geometric dimensions, was conducted by NASA in 1983 because of its potential as a reflective surface in space antennas.[27] Each edge of this membrane model was a circular arc of radius 1.41 m with a 19.05-mm Mylar hem, through which a 1.60-mm-diam steel cable was passed. The smooth surface was maintained at optical-quality flatness by transmitting uniform tension loads via the steel cables passing over the pulleys. Experimental measurements (i.e., frequencies, mode shapes, and damping coefficients) of out-of-plane vibration modes were correlated with frequencies and mode shapes calculated with SPAR, a finite element structural analysis computer program used by NASA.

The vibration analysis performed by NASA was based on an unwrinkled membrane, where the wrinkles existing near the apexes were either removed or ignored. However, this three-sided membrane model is extremely susceptible to wrinkles near the edges if the load directions are shifted by even a slight amount from their desired geometric position (passing through the membrane centroid). Therefore, the purpose of the present paper is to report a numerical investigation to determine how the basic vibration behavior differs between the unwrinkled and wrinkled configurations.

The finite element model of the three-sided membrane model consists of 1411 nodes and 1533 elements. Triangular and quadratic membrane elements, M3D3 and M3D4, respectively, available in the nonlinear finite element code ABAQUS, were used to make the membrane surface. The steel cables passing through the membrane edges, and extending beyond the apexes, were simulated by using two-node truss elements T3D2. Steel cables were bonded with membrane edges, which did not model free sliding contact between them.

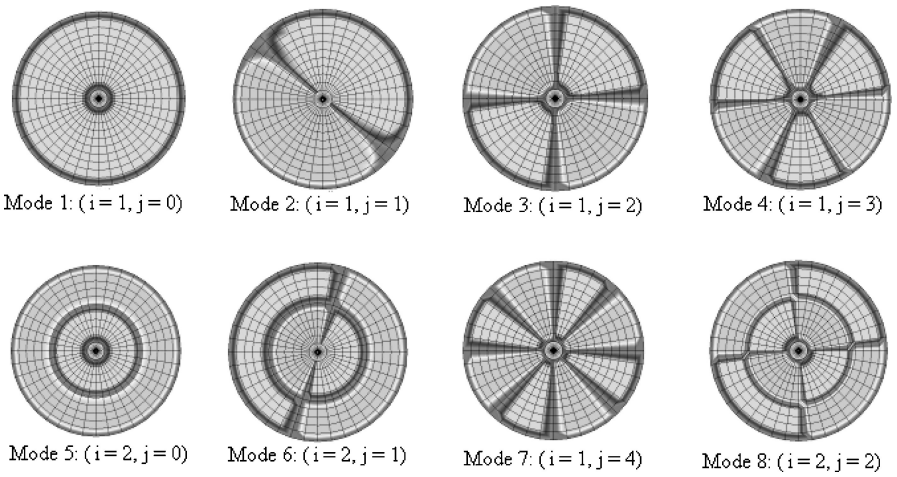

Fig. 8 Modes of vibration of uniformly pretensioned (unwrinkled) annular membrane model.

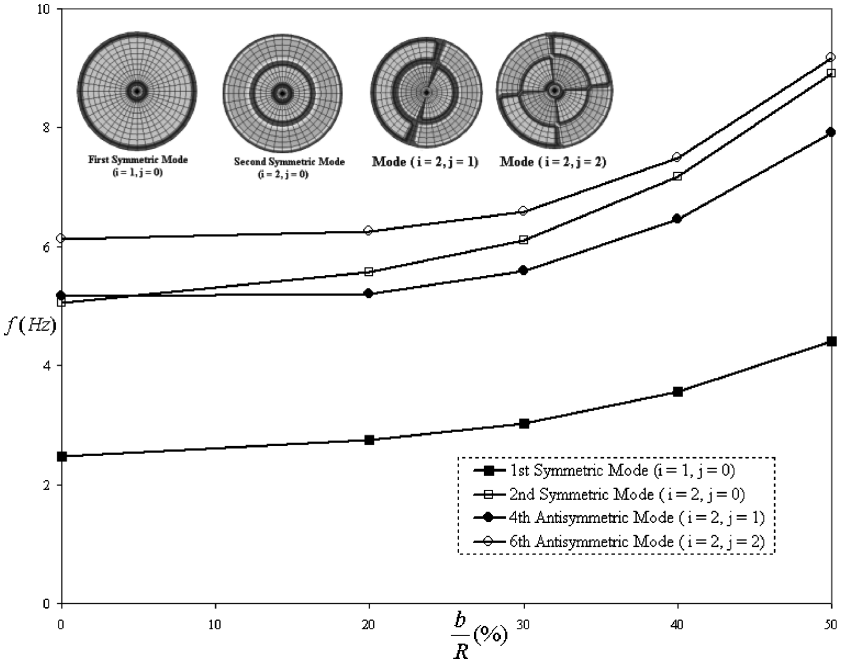

Fig. 9 Frequency of the partly wrinkled annular membrane model with increasing wrinkle radius. Symmetric and antisymmetric modes are shown.

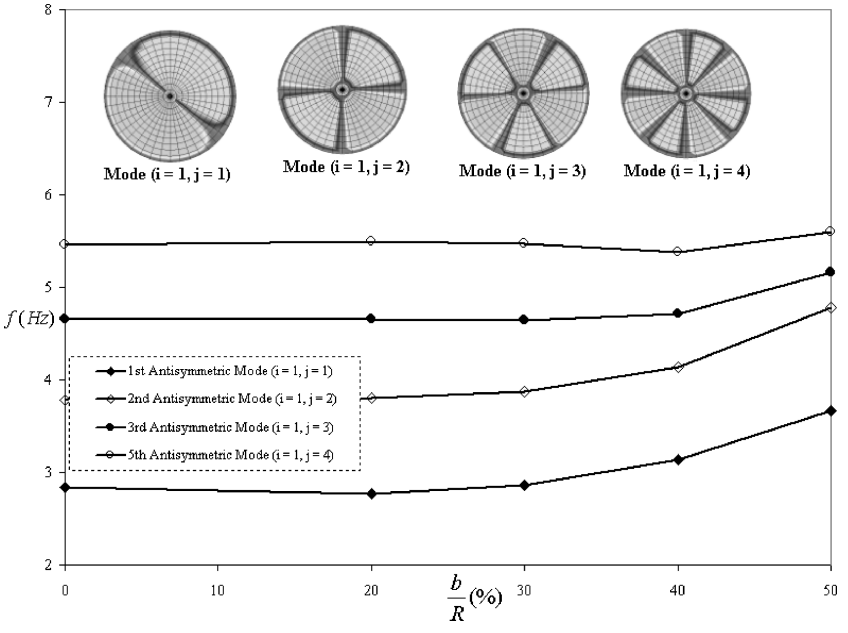

Fig. 10 Frequency of the partly wrinkled annular membrane model with increasing wrinkle radius. Antisymmetric modes with increasing the nodal diameters are shown.

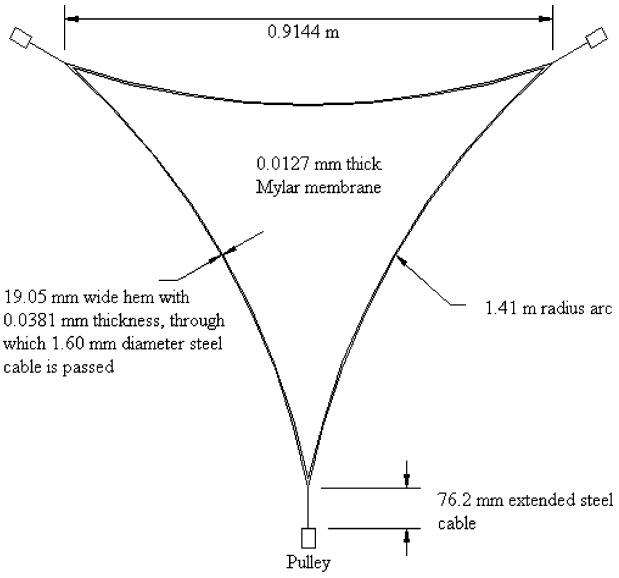

Fig. 11 Three-sided membrane model with geometric dimension (following Ref. 27).

The mass loading of the shaker was simulated as a point mass-element, MASS, of having a magnitude of 39.4 g and located at 38.1 mm below the bottom apex.

The end nodes of the extended steel cables were considered pinned during the finite element simulation, where all of the nodes of membrane edges were considered free. Thermal contraction (or thermal load) was applied at the region of extended steel cables to assign initial tension in the membrane model. The material properties used in the three-sided membrane model are shown in Table 6.

Vibration analysis of an unwrinkled three-sided membrane model, as shown in Fig. 11, was performed first to compare the ABAQUS numerical outputs with the known experimental results available in Ref. 27. Reference 27 represents the membrane experimental vibration modes and frequencies in near vacuum of 0.008 to 0.018 atmospheric pressure under three different equal apex tension loads: 93.4, 142.0, and 229.5 N. In this paper, ABAQUS analysis was performed under 142-N apex tension load and then compared with the corresponding experimental values. Mode 1 of the ABAQUS analysis is shown in Fig. 12, which indicates the first out-of-plane symmetric mode (absence of any nodal lines).

For uniform cable tension of 142 N, the first few out-of-plane vibration modes were observed and are shown in Fig. 13. For the same loading condition, these mode shapes were found to be identical to

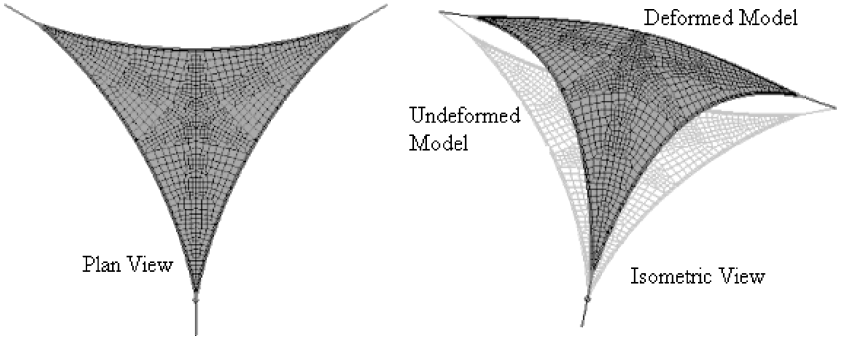

Fig. 12 Mode 1 of the unwrinkled three-sided membrane model.

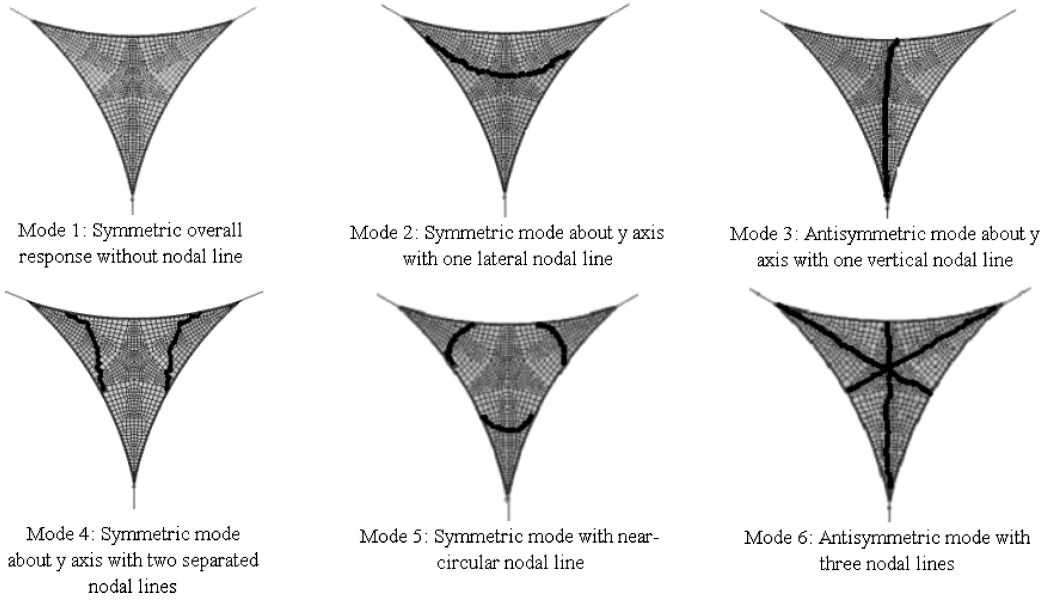

Fig. 13 Several out-of-plane vibration modes of the three-sided membrane model obtained from ABAQUS.

the mode shapes mentioned in Ref. 27. The frequency comparison among ABAQUS and experiment is shown in Table 7.

An average difference of 6.0% was found between the experimental and ABAQUS results. A small difference among the results is quite expected. For one, the ABAQUS analysis was performed under vacuum condition, where the NASA experimental analysis was completed under partial vacuum (0.008 to 0.018 atm pressure) conditions. Subsequently, for most of the cases ABAQUS frequencies were found to be a little higher than the corresponding experimental frequencies, which would be expected. In the experiment, the in-plane membrane tension was maintained by passing steel cables having free sliding capability through the membrane edges, where in the ABAQUS analysis these cables were simulated as bonded with the membrane. Because of this dissimilarity, the stress distribution in the membrane surface in the experimental model will not be precisely the same as the ABAQUS numerical model, which can also account for the frequency difference between models. Besides, experimental frequencies depend on excitation methods. For the same cable tension, a noticeable difference was observed in experimental frequencies[27] for different excitation methods. Still, a fair agreement was observed between the experimental and numerical results, except mode 2, which shows 14% difference between them. We should not lose sight of the statistical distribution of error inherent in any experiment. Hence, it was not our intension to exactly reproduce the experimental results in Ref. 27, but rather to make a reasonably accurate numerical model, which can be used for further dynamic analysis with wrinkle incorporation. Thus we take the numerical accuracy of six parts in 100 (Table 7) as an accurate baseline for this problem.

Wrinkles in this three-sided membrane model were introduced by rotating the tension cables 2 and 3 (moving nodes 1410 and 1411) from their previous geometric locations by an angle θ, as demonstrated in Fig. 14. (Such an offset might be caused by, for example, boom tip eccentricity in a solar sail.) These offset configurations were named negative (−) or positive (+) when the nominal distance between nodes 1410 and 1411 decreased or increased, respectively, because of their shifted locations. The offset amount, for example, negative or positive 7.5 deg, that was used in this analysis was chosen arbitrarily to induce a noticeable but small wrinkled area in the membrane model. The offset configuration (wrinkled) of this three-sided membrane model changed the reaction forces at the apexes compared to the original configuration (unwrinkled). Therefore, different amounts of thermal load were applied at the tension cables 2 and 3 of the wrinkled model until the reaction force at the bottom apex (node 1409) became the same as the unwrinkled model (142 N for this analysis). Also, as the out-of-plane vibration behavior of the wrinkled model was not compared with any experimental values, the effect of shaker mass was not simulated in this case. An analysis was performed in ABAQUS with and without simulating the shaker mass, where an average difference of 3% was observed.

Considered the original three-sided unwrinkled membrane model, the negative and positive 7.5-deg offset configurations were found to offer around 13 and 29% wrinkled area, respectively, which is shown in Fig. 15. A MATLAB® code was used to determine the wrinkled area in this analysis. The first few out-of-plane vibration modes for the unwrinkled and wrinkled models (for both the negative and positive offset configurations) are shown in Fig. 16. The lower-order modes of vibrations (e.g., mode nos. 1, 2, 3) were found almost the same for the unwrinkled and wrinkled membranes, where the higher-order modes were found very different from each other.

The three-sided membrane model with negative (−) or positive (+) 7.5-deg offset configuration, which shows wrinkles near the

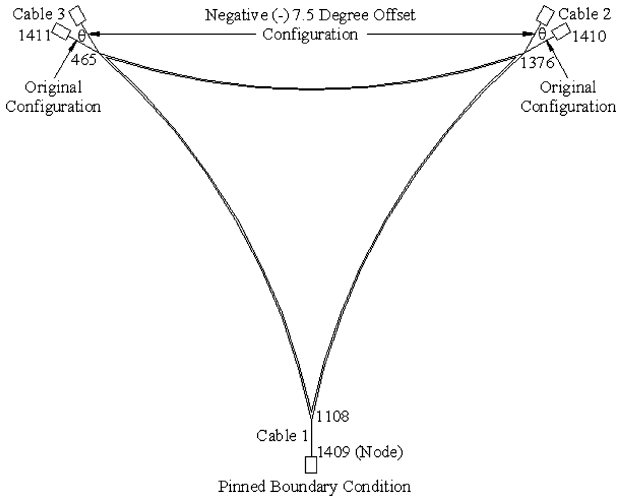

Fig. 14 Schematic view of wrinkled configuration of three-sided membrane model.

Table 6 Material properties used in three-sided membrane model

Properties	Mylar membrane	Steel cable
Modulus E	3.4 GPa	165.5 GPa
Poisson's ratio ν	0.3	0.3
Density ρ	1384 kg/m^3	5500 kg/m^3
Thermal expansion coefficient α	$2.7E-6$/°C	$1.4E-5$/°C
Thickness h or diameter d	0.0127 mm	1.60 mm

Table 7 Frequency comparison for unwrinkled three-sided membrane model between experimental results in Ref. 27 and ABAQUS analysis

Mode	NASA Expt. f_E, Hz	ABAQUS f_A, Hz	% Difference[a] $(f_E - f_A)/f_E$
1	34.25	33.55	2.04
2	48.77	55.86	−14.53
3	50.40	52.37	−3.91
4	83.36	86.54	−3.81
5	96.04	90.45	5.82
6	99.71	106.27	−6.57

[a]Average difference = 6.11.

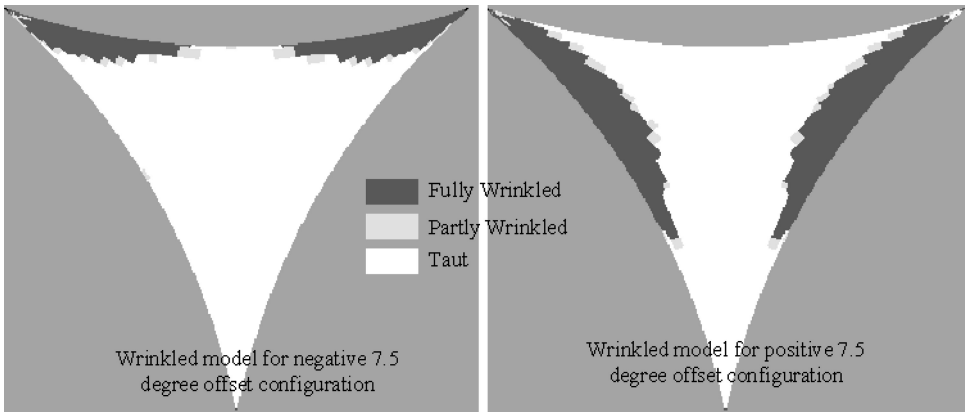

Fig. 15 Wrinkling in the three-sided membrane model for offset configuration.

Table 8 Frequency comparison for the unwrinkled and wrinkled three-sided membrane model[a]

		Negative (−) 7.5-deg offset configuration		Positive (+) 7.5-deg offset configuration	
Original unwrinkled model		Without wrinkle algorithm: frequency, Hz	With wrinkle algorithm: frequency, Hz	Without wrinkle algorithm: frequency, Hz	With wrinkle algorithm: frequency, Hz
Mode	Frequency, Hz				
1	35.22	Buckling mode	31.43	37.24	37.24
2	52.75	Buckling mode	44.24	50.48	50.51
3	52.76	31.43	52.24	Buckling mode	61.43
4	84.21	44.25	68.40	Buckling mode	79.20
5	84.21	52.28	74.26	61.50	88.02
6	89.36	68.45	81.83	72.78	95.24
7	95.93	73.88	87.00	73.82	100.30
8	107.03	81.74	99.32	78.41	113.23
9	120.23	88.37	99.72	87.81	114.79
10	125.54	99.00	101.21	93.44	122.36

[a]We compare modes if the MAC ≥ 0.75.

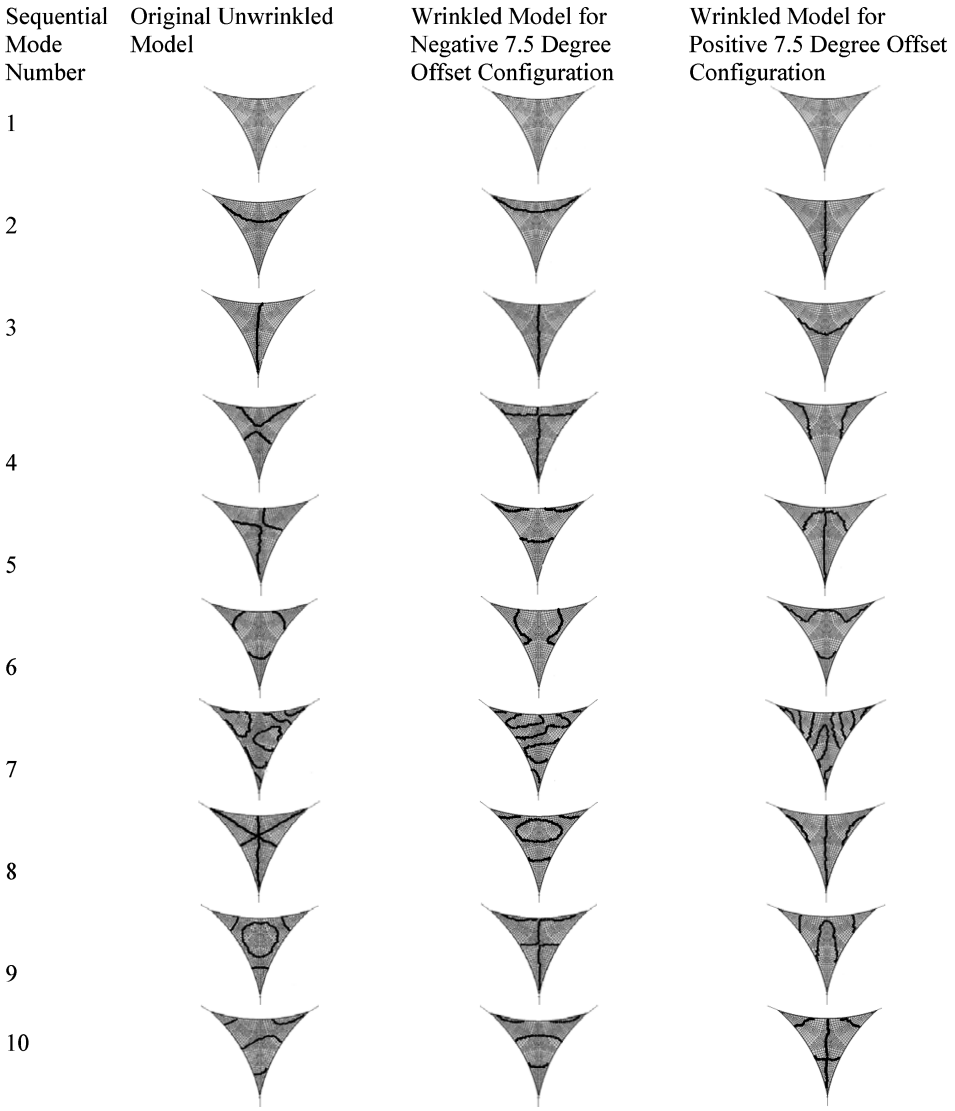

Fig. 16 Mode shapes for unwrinkled and wrinkled configurations of three-sided membrane model.

edges (see Fig. 15), was found to offer some buckling modes (modes with negative eigenvalues) when the PPMM wrinkle algorithm was not used in the analyses, likely because of the increase in compressive stress. These results are shown in Table 8. Buckling modes disappeared when the model was analyzed with the wrinkle algorithm, again likely because of the decrease in compressive stress.

Similar modes of vibrations between the unwrinkled and wrinkled models were determined by visual observation of nodal lines as well as by calculating the MAC number, as discussed earlier. (Modes of vibrations are considered here to be similar for the MAC number ≥ 0.75.) Frequency comparisons for similar modes of vibrations between the unwrinkled and wrinkled membranes are shown in Tables 9 and 10. Reaction force at the upper two tension cables (nodes 1410 and 1411) were reduced in the wrinkled model for the negative 7.5-deg offset configuration, which consequently reduced the membrane tension of the upper side. As the wrinkle

Table 9 Frequency comparison for unwrinkled and wrinkled (caused by negative offset configuration) model[a]

Unwrinkled membrane model		Wrinkled membrane model for negative 7.5-deg offset		Mode identification, MAC	% Reduction, frequency, Hz
Mode	Frequency, Hz	Mode	Frequency, Hz		
1	35.22	1	31.43	0.934	12.07
2	52.75	2	44.24	0.936	19.24
3	52.76	3	52.24	0.940	0.98
6	89.36	5	74.26	0.781	20.34
7	95.93	7	87.01	0.919	10.25

[a]PPMM wrinkle algorithm was used.

Table 10 Frequency comparison for unwrinkled and wrinkled (caused by positive offset configuration) model[a]

Unwrinkled membrane model		Wrinkled membrane model for positive 7.5-deg offset		Mode identification, MAC	% Increment, frequency, Hz
Mode	Frequency, Hz	Mode	Frequency, Hz		
1	35.22	1	37.24	0.983	5.72
2	52.75	3	61.43	0.822	16.46
3	52.76	2	50.51	0.981	−4.26
6	89.36	6	95.24	0.865	6.58
7	95.93	7	100.30	0.945	4.56

[a]PPMM wrinkle algorithm was used.

area was relatively small, the reduction in compressive stress with the PPMM wrinkle algorithm was not enough to make up for the loss of tension. Geometric stiffness was found dominant as the frequencies were reduced because of the reduction of membrane tension.

On the other hand, the wrinkled membrane model for the positive 7.5-deg offset configuration increased the reaction force at the upper two tension cables, which also increased the membrane tension of the upper side. As the wrinkle area here was over twice that of the negative 7.5-deg offset configuration, the larger reduction in compressive stress with the PPMM wrinkle algorithm contributed to the increase in frequency. As geometric stiffness increases, most of the frequencies were found to increase in this case.

In Table 9, all but one of the modes exhibited frequency changes greater than the baseline case (6%), as did two of the modes in Table 10. Thus we consider these results numerically significant.

Conclusions

A FE analysis has been presented in this paper for dynamic analysis of partly wrinkled membranes. A penalty-parameter-modified-material wrinkle algorithm was incorporated in FE analysis as a user subroutine to implement the membrane constitutive model. This wrinkle algorithm was found to offer expected results in dynamic analysis both for the annular and three-sided membrane model. In the absence of the wrinkle algorithm, frequencies of the annular membrane model decreased with the development of compressive stress. This compressive stress was minimized while using the wrinkle algorithm, and frequencies of the wrinkled model increased. For the three-sided membrane model, the wrinkled configuration developed compressive stresses, and subsequently buckling modes of vibration were observed. These buckling modes were also removed when the wrinkle algorithm was used. In effect, wrinkle reduces compressive stress (and the buckling modes) in a membrane and changes the vibration frequencies accordingly.

The change in frequencies between the unwrinkled and wrinkled models will not be the same for different modes of vibrations. Vibration modes with higher modal participation factor normal to the wrinkle plane will be affected more compared to the other modes of vibration. This statement can be supported by observing the frequency results of the wrinkled annular membrane model. Frequencies of the symmetric modes were changed significantly compared to the antisymmetric modes. As nodal lines express the stationary membrane surface, the frequency change between the unwrinkled and wrinkled models decreased with increasing the nodal circles and diameters.

The extent and orientation of the wrinkling in membranes will change the stress distribution relative to the unwrinkled case. Therefore, the wrinkled model should offer different vibration behaviors when compared to unwrinkled model. This conclusion is well supported by the cases studied here. For a particular mode of vibration, the frequency might increase or decrease from unwrinkled to wrinkled configuration depending on the net change of elastic and geometric stiffness. To draw a better and precise conclusion, a further investigation is required. For example, although the wrinkle algorithm correctly penalizes the compressive stresses, the wrinkled model might offer reduced vibration frequencies if the membrane tension is reduced by the wrinkle orientation.

We have presented, for the first time, an analysis of transverse vibration of partly wrinkled membrane based on a true membrane formulation. The use of the precisely based PPMM model correctly predicts expected membrane behavior. Furthermore, the PPMM model is robust and computationally efficient.

Acknowledgment

The authors thank NASA for partial support of this work.

References

[1]Jenkins, C. H., and Leonard, J. W., "Nonlinear Dynamic Response of Membranes: State of the Art," *Applied Mechanics Reviews*, Vol. 44, No. 7, 1991, pp. 319–328.

[2]Jenkins, C. H., Haugen, F., and Spicher, W. H., "Experimental Measurement of Wrinkling in Membranes Undergoing Planar Deformation," *Experimental Mechanics*, Vol. 38, No. 2, 1998, pp. 147–152.

[3]Wagner, H., "Flat Sheet Girder with Very Thin Metal Web," *Zeitschrift Flugtech Motorluft–Schiffahrt*, Vol. 20, 1929, pp. 200–207, 227–231, 281–284, and 306–314.

[4]Reissner, E., "On Tension Field Theory," *Proceedings of the 5th International Congress Applied Mechanics*, edited by J. P. den Hartog and H. Peters, Wiley, New York, 1938, pp. 88–92.

[5]Steigmann, D. J., and Pipkin, A. C., "Finite Deformation of Wrinkled Membranes," *Quarterly Journal Mechanics Applied Math.* Vol. 42, 1989, pp. 427–440.

[6]Roddeman, D. G., Druker, J., Oomens, C. W. J., and Janssens, J. D., "The Wrinkling of Thin Membranes: Part I—Theory," *Journal of Applied Mechanics*, Vol. 54, Dec. 1987, pp. 884–887.

[7]Roddeman, D. G., Druker, J., Oomens, C. W. J., and Janssens, J. D., "The Wrinkling of Thin Membranes: Part II—Numerical Analysis," *Journal of Applied Mechanics*, Vol. 54, Dec. 1987, pp. 888–892.

[8]Kang, S., and Im, S., "Finite Element Analysis of Wrinkling Membranes," *Journal of Applied Mechanics*, Vol. 64, No. 9, 1997, pp. 263–269.

[9]Lu, K., Accorsi, M., and Leonard, J., "Finite Element Analysis of Membrane Wrinkling," *International Journal for Numerical Methods in Engineering*, Vol. 50, No. 5, 2001, pp. 1017–1038.

[10]Nakashino, K., and Natori, M. C., "Efficient Modification Scheme of Stress-Strain Tensor for Finite Element Analysis of Wrinkling Membranes," AIAA Paper 2003-1981, April 2003.

[11]Miller, R. K., Hedgepeth, J. M., Weingarten, V. I., and Das, P., "Finite Element Analysis of Partly Wrinkled Membranes," *Computers and Structures*, Vol. 20, No. 1–3, 1985, pp. 631–639.

[12]Stein, M., and Hedgepeth, J. M., "Analysis of Partly Wrinkled Membranes," NASA TN D-813, July 1961.

[13]Mikulas, M. M., "Behavior of a Flat Stretched Membrane Wrinkled by the Rotation of an Attached Hub," NASA TN D-2456, Sept. 1964.

[14]Liu, X., Jenkins, C. H., and Schur, W. W., "Large Deflection Analysis of Pneumatic Envelopes Using a Penalty Parameter Modified Material Model," *Finite Element Analysis and Design*, Vol. 37, No. 3, 2001, pp. 233–251.

[15]Liu, X., Jenkins, C. H., and Schur, W. W., "Fine Scale Analysis of Wrinkled Membranes," *International Journal of Computational Engineering Science*, Vol. 1, No. 2, 2000, pp. 281–298.

[16]Adler, L. A., Mikulas, M. M., and Hedgepeth, J. M., "Static and Dynamic Analysis of Partly Wrinkled Membrane Structures," AIAA Paper 2000-1810, April 2000.

[17]Tessler, A., Sleight, D. W., and Wang, J. T., "Nonlinear Shell Modeling of Thin Membranes with Emphasis on Structural Wrinkling," AIAA Paper 2003-1931, April 2003.

[18]Wong, Y. W., Pellegrino, S., and Park, K. C., "Prediction of Wrinkling Amplitudes in Square Solar Sails," AIAA Paper 2003-1982, April 2003.

[19]Kukathasan, S., and Pellegrino, S., "Nonlinear Vibration of Wrinkled Membranes," AIAA Paper 2003-1747, April 2003.

[20]Jenkins, C. H., *Gossamer Spacecraft: Membrane and Inflatable Structures Technology for Space Applications*, Vol. 191, Progress in Aeronautics and Astronautics, AIAA, Reston, VA, 2001.

[21]Kondo, K., Iai, T., Moriguri, S., and Murasaki, T., "Tension Field Theory," *Memoirs of the Unifying Study of the Basic Problems in Engineering by Means of Geometry*, Vol. 1, Gakujutsu Bunken Fukyu-kai, Tokyo, 1995, pp. 61–85.

[22]Jenkins, C. H., Hossain, N. M., Woo, K., Igawa, H., Wang, J., Sleight, D., and Tessler, A., "Membrane Wrinkling," *Recent Advances in Gossamer Spacecraft*, Vol. 212, Progress in Astronautics and Aeronautics, AIAA, Reston, VA, 2005, pp. 109–163.

[23]"No Compression or No Tension Elasticity," *ABAQUS Standard User Manual*, Vol. 2, Sec. 10.2.2, ver. 6.3, Hibbit, Karlsson and Sorensen, Inc., Pawtucket, RI, 2002.

[24]"Eigenvalue Extraction," *ABAQUS Theory Manual*, Sec. 2.5.1, ver. 6.3, Hibbit, Karlsson and Sorensen, Inc., Pawtucket, RI, 2002.

[25]Blevins, R. D., "Formulas for Natural Frequencies and Mode Shape," *Membranes,* 4th ed., Krieger, Malabar, FL, 1987, pp. 224–231.

[26]Ewins, D. J., "Modal Testing: Theory, Practice and Application," *Application*, 2nd ed., Research Studies Press, Ltd., Baldock, England, U.K., 2000, pp. 422–425.

[27]Sewall, J. L., Miserentino, R., and Pappa, R. S., "Vibration Studies of a Lightweight Three-Sided Membrane Suitable for Space Application," NASA TP 2095, Jan. 1983.

G. Agnes
Associate Editor